HAVSTOVAN
FAROE MARINE RESEARCH INSTITUTE

Adapting Faroe Current monitoring to a reprocessed altimetry data set

Tórshavn · August 2023

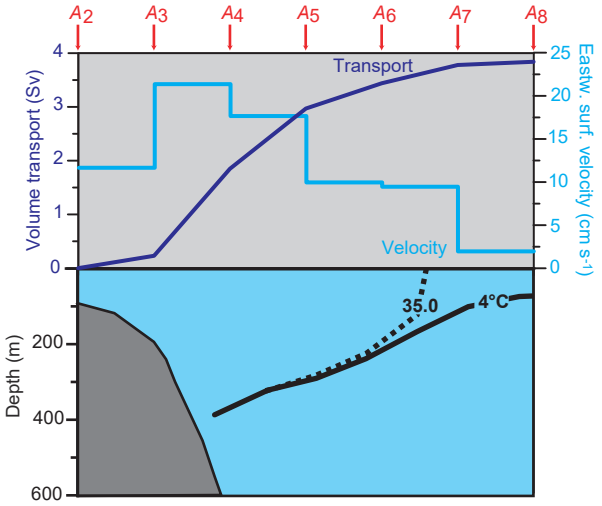

Bogi Hansen

Karin Margretha Húsgarð Larsen

Hjálmar Hátún

HAVSTOVAN NR.: 23-02
TECHNICAL REPORT

Adapting Faroe Current monitoring to a reprocessed altimetry data set

Bogi Hansen, Karin Margretha Húsgarð Larsen, and Hjálmar Hátún

The present project has been supported by the Danish Energy Agency as part of the Arctic Climate Support Programme. The authors are solely responsible for the results and conclusions presented in the report. They do not necessarily reflect the position of the Danish Energy Agency.

Abstract

The monitoring system for the Faroe Current uses available in situ observations of temperature and salinity, but also relies heavily on satellite data from eight altimetry grid points (A_1 to A_8). Using algorithms documented in a number of publications (H2015, H2019, and H2020), time series of the four monitoring parameters (volume transport of Atlantic water, heat transport relative to 0°C, and transport-averaged temperature and salinity) have been updated whenever the altimetry data set was updated. With the altimetry data update in December 2021, it was clear, however, that there were major changes in the data set; not only in the latest part, but throughout the altimetry period, beginning in 1993. This raised two main questions:

- Are the relationships, on which the algorithms are based, still valid?
- Which equations and coefficients need to be modified?

Answering these questions was the main aim of this report. The equations and algorithms have been developed by comparing altimetry data with various types of in situ observations. To answer the two questions above, we have therefore re-done the analyses, mostly in the form of regression analyses. The result was unequivocal. All the relationships were still valid and for all of them, the explanatory power increased with the new altimetry data set, although some of the coefficients had to be modified.

In this process, a number of results and conclusions of more general interest have emerged. These have been published in a scientific manuscript (Hansen et al., 2023) and the interested reader should refer to that publication. This report duplicates some of these results in more detail, but is mainly intended to provide a more detailed documentation of the monitoring system for future reference.

In spite of higher explanatory power and some coefficient modifications, the time series generated from the new altimetry data (e.g., volume transport) only differ slightly from the series generated from the old data. The new analyses also support our previous conclusion that in situ current measurements are no longer necessary to monitor the velocity structure of the Faroe Current, although we recommend that one of the long-term ADCP mooring sites is maintained to guard against potential drastic changes in the system.

1 Introduction

The inflow of Atlantic water to the Nordic Seas between Iceland and the Faroes becomes focused into a relatively narrow boundary current north of the Faroes, termed the Faroe Current (Figure 1.1). Since the late 1980s, hydrographic properties of this current have been monitored by regular CTD observations at a fixed set of standard stations N01 to N14 along a section, the N-section, that follows the 6.083°W meridian.

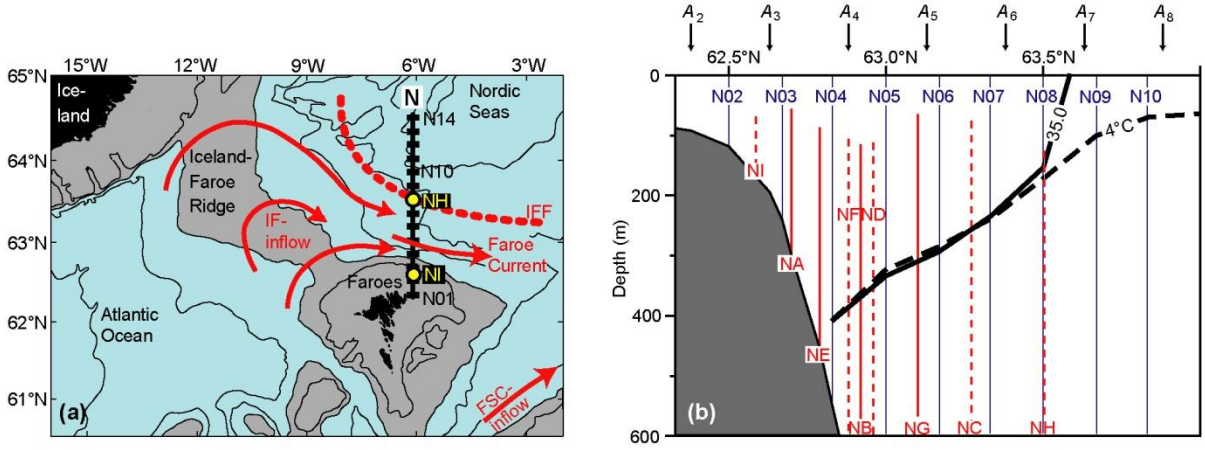

Figure 1.1. (a) The region between Iceland and the Scottish shelf with grey areas shallower than 500m. The two main Atlantic inflow branches are indicated by red arrows. The Iceland-Faroe inflow (IF-inflow) crosses the Iceland-Faroe Ridge (IFR), meets colder waters, termed Arctic water, in the Iceland-Faroe Front (IFF), and flows north of Faroes in the Faroe Current. The other main inflow branch (the FSC-inflow) is also shown. The black line extending northwards from the Faroe shelf is the N-section with CTD standard stations N01 to N14 indicated by black rectangles. Yellow circles indicate the innermost (NI) and the outermost (NH) ADCP mooring sites on the section. **(b)** The southernmost part of the N-section with bottom topography (grey). CTD standard stations are indicated by blue lines labelled N02 to N10. ADCP profiles are marked by red lines that indicate the typical range with continuous lines indicating the long-term sites. Altimetry grid points A_2 to A_8 are marked by black arrows and the thick black lines indicate the average depth of the 4 °C isotherm (dashed) and the 35.0 isohaline (continuous) on the section (from Hansen et al., 2015).

In the mid-1990s, the hydrographic observations were complemented by regular deployments of upward looking ADCPs (Acoustic Doppler Current Profilers) along the section (Figure 1.1). These deployments have mainly been repeated at some fixed sites, but in addition, single deployments have been located at other sites.

The main aim of these observations has been to monitor transports of volume (water, mass), heat, and salt in the Faroe Current and, originally, the estimated transport values were based purely on the in situ measurements (ADCP and CTD observations), but these estimates were found to correlate remarkably well with sea-level data from satellite altimetry (Hansen et al., 2010). Altimetry data and ADCP data also complement one another well and a new strategy was adopted, which is based on combining altimetry data and in situ data.

The implementation of this strategy was realized in the period 2015 to 2020 and is documented in three publications, which henceforth will be referred to as H2015, H2019, and H2020, as elaborated in the reference list. A main conclusion from these studies was that data from satellite altimetry could be used to generate volume transport time series of Atlantic water in the Faroe Current to a remarkable accuracy. Once calibrated by long-term in situ observations, transport estimates generated from altimetry solely, were found to be highly accurate, although the accuracy could be improved by additional in situ observations.

The presently adopted monitoring strategy for the Faroe Current therefore relies heavily on the altimetry data set. Usually, updates of the altimetry data have only involved adding additional data, but the update released in December 2021 also included reprocessing the whole data set from its

beginning in 1993. As detailed in Sect. 2, some of the altimetry-derived parameters in the algorithms used for transport calculation have changed markedly throughout the time series.

This has necessitated a re-evaluation of the algorithms and that is the purpose of this report. The calculation of transport may be split into three main tasks:

I. **Using altimetry data to calculate surface velocities.** By comparison with data from moored ADCPs, it was shown in H2019 that variations of eastward surface velocity on monthly time scales were highly correlated with sea level differences between altimetry grid points as given in the altimetry data set in accordance with geostrophy. Using the ADCP data and hydrographic (CTD) observations, H2019 furthermore documented that the altimetry data could be calibrated to give highly accurate absolute surface velocities (not only their variations).

II. **Determining the vertical velocity variation from surface velocity.** Calculating transport involves integration of the velocity field both horizontally and vertically and this requires knowledge of the vertical variation of the velocity. In H2019, it was documented that monthly averaged eastward velocities at a given depth may be accurately derived from surface velocity, although seasonally dependent. This implies that volume transport of Atlantic water on monthly time scales may be calculated from surface velocity and the depth of the Atlantic layer along the section as well as its northward extent.

III. **Determining the hydrographic structure and the depth of the Atlantic layer along the monitoring section**. In order to distinguish the volume transport of Atlantic water from the other water masses flowing through the monitoring section, the temporal variation of the depth of the Atlantic water layer along the section has to be derived from the available observational data. Calculating transport of heat and salt furthermore requires knowledge of the temporal variations of the temperature and salinity fields on the section. In H2020, it was documented that also the Atlantic water extent with a fair degree of accuracy may be derived from the altimetry data, although in situ observations may increase the accuracy.

The reprocessing of the altimetry data set does not affect task II, but the other two tasks need to be investigated to clarify whether the high correlations between altimetry and ADCP data survive the revision and to update the calibrations. This is reported in Sect. 3, which is followed by an appendix that summarizes the details of Faroe Current monitoring at its present stage.

The work associated with this report has been supported the Danish Energy Agency in the FARMON project.

2 Data

2.1 Altimetry data

Both the old and the new versions of the altimetry data were selected from the global gridded (0.25°x0.25°) sea level anomaly (SLA) field available from Copernicus Marine Environment Monitoring Service (CMEMS) (http://marine.copernicus.eu):

- **Old altimetry data set:** SEALEVEL_GLO_PHY_L4_REP_OBSERVATIONS_008_047
- **New altimetry data set:** SEALEVEL_GLO_PHY_L4_MY_008_047

From each of these data sets, SLA values were selected for 8 grid points, which we label A_1 to A_8, along 6.125°W from 62.125°N to 63.875°N (Figure 1.1b). For each of these points, we have analyzed sea level anomalies $H_k(t)$, k = 1 to 8, for 9629 days from 1 January 1993 to 13 May 2019 in both the old and the new versions.

In addition to the $H_k(t)$ values, other derived parameters have been used extensively. Included are seven parameters $u_k(t)$, k = 1 to 7 that should represent the eastward surface velocity horizontally averaged over each interval between two altimetry grid points according to geostrophy:

$$u_k(t) \equiv \frac{g}{f \cdot L} \cdot [H_k(t) - H_{k+1}(t)] = \frac{g}{f \cdot L} \cdot \Delta H_k(t) \qquad (1)$$

Although other altimetric parameters have been investigated, the one additional parameter generally used is the first principal component of an Empirical Orthogonal Function (EOF) analysis of the $H_k(t)$ values, termed $Pc_1(t)$. The EOF analysis is documented in H2020 (Sect. 5.2) where this parameter was termed *PcAH-1(t)* and where it is seen that this principal component explains 88% of the variance of sea level height.

Some explanation may be needed to clarify the definition of this principal component. Using a simpler notation than in H2020, an EOF analysis of $H_k(t)$ means that the values may be written as:

$$H_k(t) = \langle H_k \rangle + \sum_j M_j(k) \cdot pc_j(t) \qquad (2)$$

where $\langle H_k \rangle$ is the temporal average of $H_k(t)$, $M_j(k)$ is the j-th spatial EOF mode while $pc_j(t)$ is its associated principal component. In principle, a new EOF analysis ought perhaps to be done every time the altimetry data set is updated, but then all the relationships that use the principal components (e.g., the depth of the Atlantic layer on the section) should also be re-analyzed. To avoid that, the values for the spatial $M_j(k)$ modes are kept fixed to the values derived in Sect. 5.2 in H2020. To derive the principal components from a new data set, we employ the orthogonality of the modes, which implies:

$$Pc_i(t) = \frac{\sum_k [H_k(t) - \langle H_k \rangle] \cdot M_i(k)}{\sum_k M_i(k) \cdot M_i(k)} \qquad (3)$$

This relationship holds for all the principal components and therefore also for $Pc_1(t)$ and it is used to update this principal component at every update of the altimetry data set. In principle, the sums in Eq. (2) and Eq. (3) should be over a large number of modes, but the first modes dominate so much (Table 5.2 in H2020) that we only retain the first eight modes in Eq. (3).

As long as old values for $H_k(t)$ are not changed in an update, the old values for $Pc_1(t)$ are not changed either. With the new altimetry data from the 2021 revision, values for $H_k(t)$ have been changed throughout the altimetry period. Since we want to retain the relationships that were deduced in H2020, The EOF analysis has not been redone, however. Instead, we use the values for the first spatial mode in Eq. (3) that were derived in H2020 (where the mode was denoted MAH-1).

With eight SLA-parameters, $H_k(t)$, seven velocity parameters, $u_k(t)$, and $Pc_1(t)$, altogether sixteen altimetry parameters have been involved in the analyses in H2015, H2019, and H2020. These sixteen parameters have been generated for both the old and the new altimetry data and are discussed in this report.

2.2 ADCP data

The ADCP data have been acquired at nine separate sites along the monitoring section. The deployment sites are labelled with two-letter codes where the first letter (N) refers to the section (Table 2.1). Data from seven of these sites (the short records from site NF and site ND are excluded) were discussed in H2019 and will be used here.

The velocity data from the ADCPs are structured in "bins" (i.e. depth intervals), which in our case have been either 10 m or 25 m. Usually, the ADCPs have been programmed to ping every 20 minutes. The raw data have been processed, edited, de-tided, and averaged to daily values. The highest level with 100% "good" daily averaged data (i.e. not error flagged) is generally well below the surface, but in H2019 it is shown that the ADCP data may be extrapolated to the surface with high accuracy.

Table 2.1. Main characteristics of the measurements at the nine ADCP sites and their locations in altimetry intervals.

Site	Latitude	Bottom depth (m)	Period	Number of depl.	Number of days	Distance from N02	Altimetry interval
NI	62.58°N	156	Jun 2017 - May 2018	1	342	9 km	A_2-A_3
NA	62.70°N	300	Jun 1996 - May 2015	20	6663	22 km	A_3-A_4
NE	62.79°N	455	Jul 2000 - May 2011	8	2729	32 km	A_3-A_4
NF	62.88°N	700	Jul 2000 - Jun 2001	1	343	42 km	A_4
NB	62.92°N	925	Oct 1994 - May 2018	24	7272	47 km	A_4-A_5
ND	62.96°N	1280	Nov 1997 - Jun 1998	1	213	51 km	A_4-A_5
NG	63.10°N	1815	Jul 2000 - May 2015	14	4788	67 km	A_4-A_5
NC	63.27°N	1730	Oct 1994 - Jun 2000	5	1517	85 km	A_5-A_6
NH	63.50°N	1802	Jun 2015 - May 2016	1	339	111 km	A_6-A_7

2.3 Hydrographic data

The hydrographic (temperature and salinity) data have been gathered from CTD profiles at the standard stations (Figure 1.1), from bottom temperature loggers, especially at site NE (Figure 1.1b), and at two locations where PIES (Pressure Inverted Echo Sounders) have been moored. These data are described in detail in H2020.

2.4 Differences between the old and the new altimetry data sets

The main differences in the altimetry data on monthly time scales are listed in Table 2.2. Since the transport calculation are carried out on monthly rather than daily time scales, the comparison in Table 2.2 has been chosen for 28-day averaged data, but the results would not differ qualitatively if daily time scales were considered instead.

For the original SLA time series, $H_k(t)$, k = 1 to 8, the old and new data in Table 2.2 do not differ dramatically, but for the velocity parameters, $u_k(t)$, k = 1 to 7, there are large differences. When considering the correlation coefficients, this is especially the case for $u_1(t)$ and $u_2(t)$, but also the other velocity parameters have large differences in standard deviation and large deviations from 1 for the regression coefficients α and α_0. The least affected parameter for both the daily and the 28-day averaged data is the principal component, $Pc_1(t)$.

Table 2.2. Comparison between the characteristics of the 28-day averages of the sixteen parameters in the old and the new altimetry data sets. "Avg_O" is the average in the old data set. "Avg_N" is the average in the new data set. "Std_O" is the standard deviation in the old data set. "Std_N" is the standard deviation in the new data set. "R" is the correlation coefficient between the old and the new values with statistical significance[1]. "α" and "β" are the coefficients in the regression equation: "old=α·new+β". "α_0" is the coefficient in the regression equation: "old= α_0·new".

Param.	Unit	Avg_O	Avg_N	Std_O	Std_N	R	α	β	α_0
H_1	cm	3.4	3.3	5.4	5.4	0.980***	0.976	0.2	0.991
H_2	cm	3.4	3.3	5.2	5.3	0.980***	0.961	0.3	0.983
H_3	cm	3.5	3.4	5.2	5.0	0.982***	1.016	0.1	1.021
H_4	cm	3.6	3.5	6.0	5.9	0.984***	0.990	0.2	1.002
H_5	cm	3.7	3.5	7.1	7.5	0.988***	0.946	0.4	0.964
H_6	cm	3.7	3.5	7.5	7.5	0.991***	0.989	0.3	1.003
H_7	cm	3.7	3.5	6.9	6.7	0.991***	1.020	0.1	1.027
H_8	cm	3.6	3.5	6.4	6.1	0.990***	1.029	0.0	1.032
u_1	cm/s	0.1	0.2	1.8	2.2	0.639***	0.526	0.0	0.526
u_2	cm/s	-0.2	-0.2	2.6	3.0	0.639***	0.551	-0.0	0.552
u_3	cm/s	-0.4	-0.3	4.8	6.1	0.907***	0.715	-0.2	0.717
u_4	cm/s	-0.2	-0.2	5.7	7.5	0.949***	0.721	-0.1	0.721
u_5	cm/s	0.0	0.2	4.2	5.7	0.901***	0.665	-0.1	0.664
u_6	cm/s	0.1	-0.0	3.9	5.2	0.917***	0.683	0.1	0.683
u_7	cm/s	0.1	0.0	3.5	4.7	0.926***	0.696	0.1	0.696
Pc_1		-0.0	-0.0	1.0	1.0	0.993***	1.003	0.0	1.003

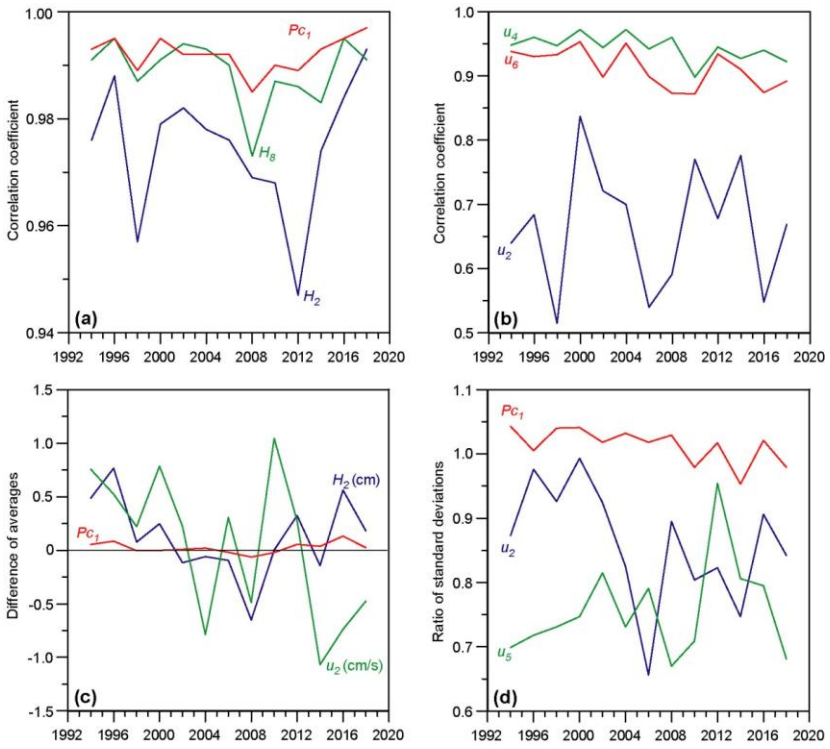

Figure 2.1. Temporal variations in the relationships between the old and the new altimetry data set through the altimetry period. The whole altimetry period was split into thirteen 2-year (730 days) periods and the characteristics in Table 2.2 were calculated for each period separately and selected features plotted against time. **(a)** Temporal variation of the correlation coefficients between old and new values for the principal component and SLA-value at two grid points. **(b)** Temporal variation of the correlation coefficients between old and new values for three of the altimetric velocity parameters. **(c)** Temporal variation of the difference between old and new averages (old minus new) for three of the altimetric parameters. **(d)** Temporal variation of the ratios between old and new standard deviations (old/new) for three of the altimetric parameters.

[1] Here and elsewhere statistical significance is indicated by asterisks: "*" indicates $p<0.05$, "**" indicates $p<0.01$, "***" indicates $p<0.001$. Significance levels are corrected for serial correlation using the "Modified Chelton method" (Pyper and Peterman, 1998).

Faced with the large discrepancies in Table 2.2, a likely explanation might be changes in instrumentation or calibration of the altimetry data during the altimetry period. To look for this kind of changes, we have split the altimetry period into thirteen non-overlapping 2-year periods and re-done the calculations of Table 2.2 for each of these shorter periods. The result is illustrated for selected parameters in Figure 2.1, but no clear picture emerges.

3 Checking and adapting calibration of volume transport calculation

As elaborated in H2019 and H2020, calculation of Atlantic water volume transport, *Q(t)*, in the Faroe Current is based on horizontal and vertical integration along the altimeter track extending northwards along the 6.125°W longitude:

$$Q(t) = \sum_{k=2}^{7} \sum_{z=1m}^{500m} U_k(z,t) \cdot W_k(z,t) \qquad (4)$$

where $U_k(z,t)$ is the eastward velocity at depth z and time t horizontally averaged within altimetry interval k, which spans $A_k - A_{k+1}$. $W_k(z,t)$ is the width of altimetry interval k at depth z and time t. When the whole interval is within the Atlantic water domain, the width is equal to the distance between the two altimetry points at each end of it. At greater depth, the width starts to decrease when the bottom or the deep boundary of the Atlantic layer is reached and falls to zero at depths where the whole interval is below the deep Atlantic water boundary or the bottom. Similarly, the width is reduced when the northern boundary enters the interval. As shown in H2019, the velocity at depth z and time t may to a good approximation be written as:

$$U_k(z,t) = \Phi_{k,m}(z) \cdot U_k(0,t) \qquad (5)$$

where the proportionality factor, $\Phi_{k,m}(z)$, for each altimetry interval, k, and month, m, was determined in H2019. $U_k(0,t)$ is the horizontally averaged eastward surface ($z = 0$) velocity between grid points A_k and A_{k+1}. If we assume geostrophic balance, $U_k(0,t)$ is proportional to the difference in absolute sea level height (SLH) between the two points A_k and A_{k+1}. The SLA values, $H_k(t)$, do not represent absolute SLH (above the geoid), but rather the anomaly. The surface velocities, $u_k(t)$, derived directly from SLA differences between two grid points are therefore also anomalies, but may be made absolute by adding a constant ***"Altimetric offset"*** U_k^0 for each interval:

$$U_k(0,t) = u_k(t) + U_k^0 = \frac{g}{f \cdot L} \cdot [H_k(t) - H_{k+1}(t)] + U_k^0 = \frac{g}{f \cdot L} \cdot \Delta H_k(t) + U_k^0 \qquad (6)$$

where g and f are gravity and Coriolis parameter, respectively, and L is the distance between the altimetry grid points and we have defined: $\Delta H_k(t) \equiv [H_k(t) - H_{k+1}(t)]$. Combining Eq. (5) and Eq.(6), we get:

$$U_k(z,t) = \Phi_{k,m}(z) \cdot U_k(0,t) = \Phi_{k,m}(z) \cdot \left[\frac{g}{f \cdot L} \cdot \Delta H_k(t) + U_k^0\right] \qquad (7)$$

In H2019, it was shown that there were fairly high correlation coefficients between values of $\Delta H_k(t)$ and observed surface velocity from ADCP data extrapolated to the surface on monthly time scales, when taking into account the difference between the horizontally localized ADCP velocities and the horizontally averaged values for $U_k(0,t)$. It was, however, also found that the regression coefficients generally were somewhat higher than the theoretical value, $g/(f \cdot L)$, based on geostrophy.

In spite of this, the theoretical values have been used as in Eq. (7) and values for the constants U_k^0 for each altimetry interval were determined in the region between altimetry points A_2 and A_8 based on the available ADCP data and average baroclinic profiles that were derived from the CTD data.

From Table 2.2, it is clear, however, that the new altimetry data set differs considerably from the old set. In the following section, we therefore first repeat the analysis in H2019 to check how good the correspondence is between altimetry and ADCP data and update the values for the Altimetric offset U_k^0 for each interval.

3.1 Using ADCP observations to check and calibrate altimetry-derived surface velocities

In H2019, correlation coefficients were determined between $\Delta H_k(t)$ and ADCP velocities extrapolated to the surface. Table 3.1a is a copy of the original Table 4a in H2019. In Table 3.1b, the analysis is repeated with the new altimetry data.

Table 3.1a: Old altimetry data. Correlation coefficients between 28-day averaged values for eastward surface velocities from ADCPs and differences in SLA values between two neighbouring points, $\Delta H_k(t)$. Correlation coefficients are bold and underlined when the ADCP site is within the interval between the two altimetry points. If the site is close to one of the points, the closest neighbouring interval is also shown in bold (but not underlined). The second column (N) indicates the number of 28-day periods used for calculation of each correlation coefficient.

Site	N	A_1-A_2	A_2-A_3	A_3-A_4	A_4-A_5	A_5-A_6	A_6-A_7	A_7-A_8
NI	12	0.34	**0.42**	-0.11	-0.17	0.14	0.18	0.03
NA	231	0.16	**0.62*****	**0.28*****	-0.18	-0.45***	-0.20**	0.06
NE	95	-0.23	0.51***	**0.78*****	0.36*	-0.31*	-0.53***	-0.27*
NB	253	-0.29**	0.17*	**0.76*****	**0.73*****	0.08	-0.60***	-0.55***
NG	167	-0.16	-0.46***	0.05	**0.61*****	**0.67*****	-0.12	-0.46***
NC	53	-0.06	-0.30*	-0.24	-0.01	**0.39****	0.35**	0.02
NH	12	0.33	0.07	-0.19	-0.20	0.25	**0.65***	0.36

Table 3.1b: New altimetry data. Correlation coefficients between 28-day averaged values for eastward surface velocities from ADCPs and differences in SLA values between two neighbouring points, $\Delta H_k(t)$. Correlation coefficients are bold and underlined when the ADCP site is within the interval between the two altimetry points. If the site is close to one of the points, the closest neighbouring interval is also shown in bold (but not underlined). The second column (N) indicates the number of 28-day periods used for calculation of each correlation coefficient.

Site	N	A_1-A_2	A_2-A_3	A_3-A_4	A_4-A_5	A_5-A_6	A_6-A_7	A_7-A_8
NI	12	0.05	**0.67**	-0.08	-0.30	0.25	0.14	-0.17
NA	231	-0.10	**0.56*****	**0.39*****	-0.22*	-0.36***	-0.09	0.04
NE	95	-0.16	0.10	**0.84*****	0.35*	-0.48***	-0.40**	-0.08
NB	253	-0.08	-0.23*	**0.65*****	**0.77*****	-0.17*	-0.57***	-0.36***
NG	167	0.03	-0.35***	-0.17*	**0.62*****	**0.62*****	-0.34***	-0.39***
NC	53	-0.03	-0.20	-0.25	-0.11	**0.42****	0.39**	-0.04
NH	12	-0.13	0.47	0.01	-0.39	0.08	**0.85*****	0.13

For each of the ADCP sites, the underlined bold values in Table 3.1 represent the altimetry interval in which the site is located. Comparing Table 3.1a and Table 3.1b for these cases, it is seen that the correlation coefficient increases in every case when changing from the old to the new altimetry data.

For these cases, the regression coefficients between $\Delta H_k(t)$ and ADCP velocities extrapolated to the surface were listed in Table 4b in H2019. This table is copied in Table 3.2a, below together with Table 3.2b, which has the same information using the new altimetry data. Consistent with higher correlations, the regression parameters tend to have smaller confidence intervals in Table 3.2b than in Table 3.2a.

Table 3.2a: Old altimetry data. Correlation and regression coefficients between 28-day averaged values for eastward surface velocities from ADCPs and differences in SLA values between the two neighbouring altimetry points that straddle the ADCP location. The last two columns list the coefficients in the regression equation $U(0,t) = a \cdot \Delta H(t) + b$ with 95% confidence intervals[2].

Site	Altimetry	Correl.	a (s^{-1})	b (cm s^{-1})
NI	A_2-A_3	0.42	2.4 ± 3.8	12.4 ± 3.0
NA	A_3-A_4	0.28***	1.2 ± 0.6	18.2 ± 1.0
NE	A_3-A_4	0.78***	5.0 ± 0.8	24.3 ± 1.4
NB	A_4-A_5	0.73***	4.3 ± 0.5	22.7 ± 1.1
NG	A_4-A_5	0.61***	3.1 ± 0.6	12.6 ± 1.3
NC	A_5-A_6	0.39**	2.1 ± 1.4	8.6 ± 1.9
NH	A_6-A_7	0.65*	5.7 ± 4.7	10.1 ± 5.0

[2] Here and elsewhere, the 95% confidence intervals are the standard errors multiplied by 1.96, corrected for serial correlation by replacing the sample size by the "equivalent sample size" (von Storch, 1999) calculated from the autocorrelation of the time series.

Table 3.2b: New altimetry data. Correlation and regression coefficients between 28-day averaged values for eastward surface velocities from ADCPs and differences in SLA values between the two neighbouring altimetry points that straddle the ADCP location. The last two columns list the coefficients in the regression equation $U(0,t) = a \cdot \Delta H(t) + b$ with 95% confidence intervals.

Site	Altimetry	Correl.	a (s^{-1})	b (cm s^{-1})
NI	A_2-A_3	0.67	2.8 ± 2.7	12.7 ± 3.0
NA	A_3-A_4	0.39***	1.3 ± 0.4	18.2 ± 1.0
NE	A_3-A_4	0.84***	4.1 ± 0.6	24.2 ± 1.2
NB	A_4-A_5	0.77***	3.4 ± 0.4	22.6 ± 1.0
NG	A_4-A_5	0.62***	2.3 ± 0.5	12.5 ± 1.3
NC	A_5-A_6	0.42**	1.7 ± 1.0	8.4 ± 1.9
NH	A_6-A_7	0.85***	4.9 ± 2.2	10.1 ± 3.4

To emphasize the difference between the two altimetry data sets, the information in Table 3.1 and Table 3.2 is summarized in Table 3.3, which again shows that the new data set gives higher correlations and tends to give smaller confidence intervals.

Table 3.3. Comparison between correlation and regression coefficients based on old and new altimetry data. "R" is the correlation coefficient between 28-day averaged values for eastward surface velocities from ADCPs and differences in SLA values between the two neighbouring altimetry points that straddle the ADCP location. "*a*" and "*b*" are the coefficients in the regression equation $U(0,t) = a \cdot \Delta H(t) + b$ with 95% confidence intervals. The theoretical value for "*a*" is based on Eq. (8).

	R		a (s^{-1})			b (cm s^{-1})	
Site	Old	New	Old	New	Theor.	Old	New
NI	0.42	0.67	2.4 ± 3.8	2.8 ± 2.7	2.72	12.4 ± 3.0	12.7 ± 3.0
NA	0.28***	0.39***	1.2 ± 0.6	1.3 ± 0.4	2.72	18.2 ± 1.0	18.2 ± 1.0
NE	0.78***	0.84***	5.0 ± 0.8	4.1 ± 0.6	2.72	24.3 ± 1.4	24.2 ± 1.2
NB	0.73***	0.77***	4.3 ± 0.5	3.4 ± 0.4	2.71	22.7 ± 1.1	22.6 ± 1.0
NG	0.61***	0.62***	3.1 ± 0.6	2.3 ± 0.5	2.71	12.6 ± 1.3	12.5 ± 1.3
NC	0.39**	0.42**	2.1 ± 1.4	1.7 ± 1.0	2.71	8.6 ± 1.9	8.4 ± 1.9
NH	0.65*	0.85***	5.7 ± 4.7	4.9 ± 2.2	2.70	10.1 ± 5.0	10.1 ± 3.4

Table 3.3 also lists the theoretical value for the regression coefficient *a* based on geostrophy, Eq. (8). For most of the ADCP sites (except site NC), the new value for regression coefficient *a* is as close or closer to the theoretical value than the old value.

$$a_{Theory} = \frac{g}{f \cdot L} \qquad (8)$$

In spite of the improvement that comes from using the new altimetry data set (Table 3.3), the "new" correlation coefficients in Table 3.3 are still in most cases well below 1 and the theoretical value for *a* is not always within the confidence interval of the regression coefficient.

A priori, this is depressing, but, as argued in H2019, it was to be expected because an ADCP measures the velocity profile at one location whereas the sea level difference between two altimetry points depends on the horizontally averaged surface velocity between the two points even with perfect geostrophy. This is illustrated by the fact that correlations between surface velocities at two neighbouring ADCPs generally are as low as or lower than the values in Table 3.3 (Table 5 in H2019).

Following the strategy in H2019, appropriate values for the U_k^0 constants are based on Eq. (9):

$$U_k^0 = \langle U_k(0,t) - \frac{g}{f \cdot L} \cdot \Delta H_k(t) \rangle \qquad (9)$$

where $\langle \quad \rangle$ indicates temporal averaging. For each ADCP site, we use daily averaged eastward surface velocity from the extended ADCP profiles to represent $U_k(0,t)$ and simultaneous SLA values to represent the difference in sea level across the altimetry interval containing the ADCP site, $\Delta H_k(t)$. Resulting values for U_k^0 using the new altimetry data set are listed together with confidence intervals in the bottom row of Table 3.4:

Table 3.4. Characteristics of observed eastward surface velocities at the nine ADCP sites as well as values for U_k^0 and their 95% confidence intervals determined from the ADCP sites within each altimetry interval using the new altimetry data set. The lowest three rows are in cm s^{-1}.

Interval:	A_2-A_3	A_3-A_4		A_4-A_5		A_5-A_6	A_6-A_7
ADCP site:	NI	NA	NE	NB	NG	NC	NH
Days:	342	6663	2729	7272	4788	1517	339
Average:	12.1	18.1	24.8	22.2	11.9	8.8	8.3
Std.dev.:	9.6	14.7	18.9	20.8	20.7	16.6	16.8
U_k^0:	12.6±2.0	18.2±2.1	24.4±2.0	22.6±1.4	12.5±1.6	7.8±2.1	9.3±3.9

The values for U_k^0 in Table 3.4 differ very little from the values in H2019 (their Table 6), but in some cases (especially for NB and NH) there are reductions in the confidence interval of significant magnitude to merit updating Figure 10 in H2019. This is done in Figure 3.1, below.

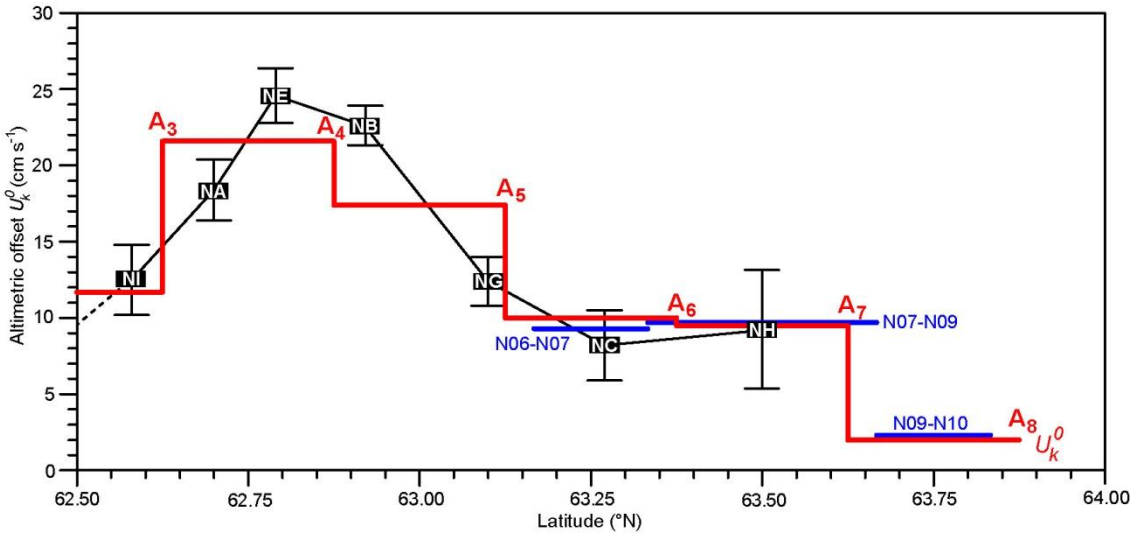

Figure 3.1. The chosen values for the Altimetric offset for surface velocity in each altimetry interval are shown by the red lines. Black rectangles with ADCP site names indicate U_k^0 values with error bars indicating 95% confidence intervals (Table 3.4) for individual ADCP sites derived from the new altimetry data set. Blue lines indicate U_k^0 values derived from CTD data and measurements of deep currents (see H2019).

In altimetry interval A_3-A_4, there are two ADCP sites, NA and NE. In addition, site NB is quite close (Figure 3.1) and is well correlated with it (Table 3.1). We therefore should be able to approximate the horizontally averaged surface velocity in this interval, $U_3(0,t)$, as a linear combination of surface velocities from these ADCPs:

$$U_3(0,t) \cong \gamma_{NA} \cdot U_{NA}(0,t) + \gamma_{NE} \cdot U_{NE}(0,t) + \gamma_{NB} \cdot U_{NB}(0,t) \qquad (10)$$

where we require that $\gamma_{NA} + \gamma_{NE} + \gamma_{NB} = 1$ to indicate that each of the three ADCP sites represents a fraction of the altimetry interval. To determine the optimal combination of coefficients, we use a "least squares" approach, varying each of the coefficients γ_{NA}, γ_{NE}, and γ_{NB} between 0 and 1 under the constraint above and minimizing the standard deviation of the residual:

$$Res(t) = \gamma_{NA} \cdot U_{NA}(0,t) + \gamma_{NE} \cdot U_{NE}(0,t) + \gamma_{NB} \cdot U_{NB}(0,t) - \frac{g}{f \cdot L} \cdot \Delta H_3(t) \qquad (11)$$

Once the optimal values for the coefficients γ_{NA}, γ_{NE}, and γ_{NB} are determined, U_3^0 is estimated as the temporal average of the residual

$$U_3^0 = \langle Res(t) \rangle = \langle \gamma_{NA} \cdot U_{NA}(0,t) + \gamma_{NE} \cdot U_{NE}(0,t) + \gamma_{NB} \cdot U_{NB}(0,t) - \frac{g}{f \cdot L} \cdot \Delta H_3(t) \rangle \qquad (12)$$

The optimal combination of coefficients found in H2019, using the old altimetry data set, is listed in the top row of Table 3.5 together with the estimated value for U_3^0. In the bottom row, the values found from the new altimetry data set are listed. To check the validity of this approach, we have generated a series of 28-day averaged values (94 values) for $U_3(0,t)$ using the determined values of γ_{NA}, γ_{NE}, and γ_{NB} and the corresponding series of 28-day averaged values for $\Delta H_3(t)$. For both the old and the new data, Table 3.5 lists the correlation coefficient between these two series as well as the coefficient a_3 in the linear regression equation:

$$U_3(0,t) = a_3 \cdot \Delta H_3(t) + b_3 \qquad (13)$$

Table 3.5. Optimal values for the three coefficients in Eq. (10) together with the estimated value for U_3^0 with its 95% confidence interval. "N_{28}" is the number of contiguous 28-day periods in the combined data set. "R_{28}" is the correlation coefficient between 28-day averaged values for $U_3(0,t)$ and $\Delta H_3(t)$. "a_3" is the regression coefficient in Eq. (13) and "$a_{Theor.}$" is the theoretical coefficient given by Eq. (8) assuming geostrophy.

Altimetry data	N_{28}	γ_{NA}	γ_{NE}	γ_{NB}	U_3^0 (cm s^{-1})	R_{28}	a_3 (s^{-1})	$a_{Theor.}$ (s^{-1})
Old data set	94	0.31	0.32	0.37	21.6 ± 1.1	0.82***	3.69 ± 0.53	2.72
New data set	94	0.33	0.34	0.33	21.4 ± 1.0	0.86***	2.87 ± 0.36	2.72

As seen in Table 3.5, the correlation coefficient between the two series increased from R_{28} = 0.82*** to R_{28} = 0.86***, when using the new altimetry data. More remarkably, perhaps, the regression coefficient a_3 became much closer to the theoretical value given by geostrophy. With the new altimetry data, the theoretical value is within the confidence interval of the regression coefficient.

A similar approach may be used for the interval A_4-A_5, which includes two ADCP sites, NB and NG. Thus, we assume that the eastward surface velocity, horizontally averaged within interval A_4-A_5 may be expressed as a linear combination of the surface velocities from ADCP sites NB and NG:

$$U_4(0,t) = \beta_{NB} \cdot U_{NB}(0,t) + \beta_{NG} \cdot U_{NG}(0,t) \qquad (14)$$

where we again require that $\beta_{NB} + \beta_{NG} = 1$. To determine the optimal combination, we again use a "least squares" approach. As demonstrated in Table 3.6, the correlation coefficient again increases with the use of the new altimetry data set and the regression coefficient becomes consistent with the theoretical value.

Table 3.6. Optimal values for the two coefficients in Eq. (14) together with the estimated value for U_4^0 with its 95% confidence interval. "N_{28}" is the number of contiguous 28-day periods in the combined data set. "R_{28}" is the correlation coefficient between 28-day averaged values for $U_4(0,t)$ and $\Delta H_4(t)$. "a_4" is the regression coefficient and "$a_{Theor.}$" is the theoretical coefficient given by Eq. (8) assuming geostrophy.

Altimetry data	N_{28}	β_{NB}	β_{NG}	U_4^0 (cm s^{-1})	R_{28}	a_4 (s^{-1})	$a_{Theor.}$ (s^{-1})
Old data set	166	0.51	0.49	17.4 ± 0.9	0.89***	3.69 ± 0.30	2.71
New data set	166	0.53	0.47	17.7 ± 0.7	0.92***	2.89 ± 0.20	2.71

As a final check, we repeat the procedure in H2019 to generate an ADCP-based time series of horizontally averaged eastward surface velocity for the combined interval A_3-A_5, through which most of the Atlantic water volume transport passes. This is done by combining Eq. (10) and Eq. (14) with the determined values for the coefficients γ_{NA}, γ_{NE}, γ_{NB}, β_{NB}, and β_{NG}:

$$U_{3+4}(0,t) = ½ \cdot [0.33 \cdot U_{NA}(0,t) + 0.34 \cdot U_{NE}(0,t) + 0.86 \cdot U_{NB}(0,t) + 0.47 \cdot U_{NG}(0,t)] \qquad (15)$$

Using 28-day averaged values, this series was correlated with the SLA difference across the combined interval, $\Delta H_{3+4}(t) \equiv [H_3(t) - H_5(t)]$ and the coefficients in the regression equation Eq. (16) were determined using the new altimetry data set.

$$U_{3+4}(0,t) = a_{3+4} \cdot \Delta H_{3+4}(t) + b_{3+4} \qquad (16)$$

The results are listed in the bottom row of Table 3.7, while the top row shows the equivalent values from H2019 (with slightly different values for the coefficients γ_{NA}, γ_{NE}, γ_{NB}, β_{NB}, and β_{NG}). Again, we find that the new altimetry data set gives higher correlation and a regression coefficient much closer to the theoretical value. This is also reflected in the difference between Figure 3.2a and Figure 3.2b where it is seen that the red squares in Figure 3.2b have a weaker tendency to slope away from the diagonal line.

Table 3.7. Correlation and regression coefficients between $U_{3+4}(0,t)$ as defined by Eq. (15) and $\Delta H_{3+4}(t)$ using both the old and the new altimetry data. "N_{28}" is the number of contiguous 28-day periods in the combined data set. "R_{28}" is the correlation coefficient between 28-day averaged values. "a_{3+4}" and "b_{3+4}" are the regression coefficients with 95% confidence intervals. "$a_{Theor.}$" is the theoretical coefficient given by Eq. (8) assuming geostrophy.

Altimetry data	N_{28}	R_{28}	a_{3+4} (s^{-1})	$a_{Theor.}$ (s^{-1})	b_{3+4} (cm s^{-1})
Old data set	94	0.86***	1.72 ± 0.21	1.36	19.5 ± 0.7
New data set	94	0.89***	1.41 ± 0.15	1.36	19.3 ± 0.6

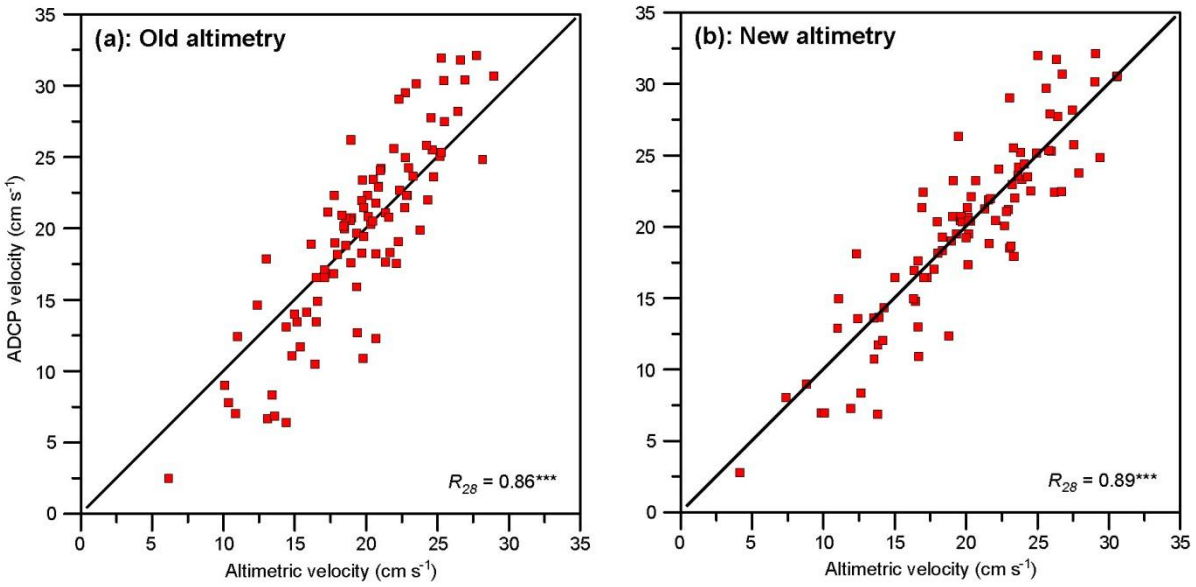

Figure 3.2. Each panel compares two different estimates of eastward surface velocity horizontally averaged between altimetry points A_3 and A_5 with the old **(a)** and the new **(b)** altimetry data sets. Each square represents a 28-day average with the value based on altimetry along the abscissa and the value based on ADCP measurements, Eq. (15) or the equivalent in H2019, along the ordinate. The diagonal line indicates equality. The altimetry-based estimates use the values for b_{3+4} from Table 3.7, but $a_{Theor.}$ rather than a_{3+4}.

Thus, we conclude that *the velocity generated from altimetry data after calibration by in situ ADCPs explains 80% (0.894^2) of the variance in the real surface velocity horizontally averaged between A_3 and A_5 on monthly time scales*. For other parts of the section, we don't have a similar amount of in situ data to check the validity of altimetry, but there does not appear to be any good reason why it should perform much worse. We therefore also conclude that *the adopted monitoring strategy, which is based on estimating surface velocity from altimetry data, calibrated by in situ measurements, is solidly based*.

3.2 Linking baroclinic velocity from CTD cruises with altimetry

In H2019, the traditional dynamical method was used on CTD data from the standard stations to calculate the velocity difference $U_{Bc}(z,t)$ between the surface and a deeper level, z, which was chosen to be at 600 m depth. For two standard stations that are between altimetry points A_k and A_{k+1}, the Altimetric offset for that interval may be estimated from an expression similar to Eq. (9):

$$U_k^0 = \langle U_{Bc}(600,t) - \frac{g}{f \cdot L} \cdot \Delta H_k(t) \rangle + \langle U_k(600,t') \rangle \equiv \langle X \rangle_g + \langle Y \rangle_{600} \qquad (17)$$

where ⟨ ⟩ again indicates temporal averaging and we have used two different averages and two different time labels (t and t') to indicate that the baroclinic velocity difference $U_{Bc}(600,t)$ and the velocity at 600 m depth $U_k(600,t')$ usually have not been measured at the same time.

For this method to be meaningful, the two parameters $U_{Bc}(600,t)$ and $\Delta H_k(t)$ have to be positively correlated. In H2019, this method was used for the three northernmost altimetry intervals and Table 3.8 verifies that the correlations using the old altimetry data were positive and highly significant. This analysis has now been repeated using the new altimetry data set and, as for the comparison with ADCP data, all the correlation coefficients increase with the use of the new data set.

Table 3.8. Comparison between baroclinic velocity differences and satellite altimetry. "N" is the number of baroclinic profiles in each CTD station interval in the altimetry period (since 1993). "R" is the correlation coefficient between $U_{Bc}(600,t)$ and $\Delta H_k(t)$ with statistical significance level. The values denoted by <X>g are defined in Eq. (17) and are listed as averages and their 95% confidence intervals. The values in the last column are based on ADCP measurements at site NC for interval A_5-A_6 and at site NH for interval A_6-A_7.

			Old altimetry data		New altimetry data		
Alt.interval	CTD st.	N	R	$\langle X \rangle_g$ cm/s	R	$\langle X \rangle_g$ cm/s	$\langle Y \rangle_{600}$ cm/s
A_5-A_6	N06-N07	99	0.50***	9.1±2.3	0.58***	8.9±2.2	0.2±1.8
A_6-A_7	N07-N09	99	0.66***	9.4±1.4	0.73***	9.2±1.3	0.3±2.7
A_7-A_8	N09-N10	96	0.44***	2.0±1.5	0.56***	2.2±1.4	

3.3 The Altimetric offsets

For the transport calculations, an important result of the previous analysis is the set of updated values for the Altimetric offsets U_k^0 for k = 2–7 to replace the values in table 8 of H2019. The changes are very small and the updated values are listed in Table 3.9 where the values that have been (slightly) changed are in bold. In addition to the "Surface" U_k^0 values that have been derived here, Table 3.9 also includes "Transport" U_k^0 values that are more suitable for transport calculations.

Table 3.9. Values for the Altimetric offset U_k^0 (in cm s^{-1}) between points A_2 and A_8. "Surface" U_k^0 values are the new values that give the best fit for the surface velocity. "Transport" U_k^0 values are adjusted for horizontal velocity variations within altimetry intervals to give values that may be more suitable for calculating volume transport as described in Sect. 3.7 of H2019.

Interval:	A_2-A_3	A_3-A_4	A_4-A_5	A_5-A_6	A_6-A_7	A_7-A_8
"Surface" U_k^0:	11.7	**21.4**	**17.7**	10	9.5	2
"Transport" U_k^0:	12.5	**21.7**	**18.0**	10	9.5	2

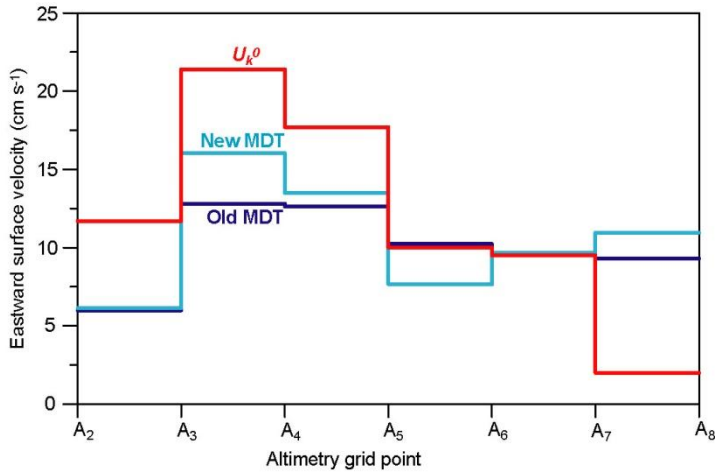

Figure 3.3. The red line shows the new values for U_k^0 based on the ADCP and CTD observations. The other two lines show the values for $U^0_{MDT,k}$ that would follow from using either the old (dark blue) or the new (cyan) published Mean Dynamic Topography (MDT) together with Eq. (18).

The good correlations found between SLA-values and extrapolated ADCP observations as well as the good correspondence between a_{3+4} and a_{Theor} in Table 3.7 indicate both fairly accurate altimetry data and geostrophic balance on long time scales. We have therefore also estimated values U_k^0 that were derived from the Mean Dynamic Topography (MDT), Z_k, along the altimetry track (which were calculated by subtracting SLA values from the associated values for Absolute Dynamic Topography):

$$U_{MDT,k}^0 = \frac{g}{f \cdot L} \cdot [Z_k - Z_{k+1}] \qquad (18)$$

In H2015, it was concluded that these values diverged too much from the values derived from ADCP observations to be realistic. In Figure 3.3, the $U_{MDT,k}^0$ values derived from the same MDT values as in H2015 are shown in dark blue, whereas the red line is based on the in situ observations (Table 3.9). Clearly, there are large differences. If we use the MDT values associated with the new altimetry data set (cyan line), the differences decrease, especially in the core of the current, but there is still a large discrepancy between the red and the cyan line. The effect of these different options on the average volume transport is documented in Table 3.10. Even with the new MDT, the average volume transport would have been severely underestimated

Table 3.10. The average volume transport and heat transport relative to 0°C of Atlantic water 1993-2018 calculated with three different choices for the altimetric offsets.

	U_k^0 from Table 3.9	$U_{MDT,k}^0$ using old MDT	$U_{MDT,k}^0$ using new MDT
Volume transport:	3.81 Sv	2.78 Sv	2.99 Sv
Heat transport:	124.8 TW	90.9 TW	97.8 TW

3.4 The Atlantic water extent

Once the velocity field has been determined, the remaining task for calculating volume transport is to derive values for the $W_k(z,t)$ parameter in Eq. (4). South of standard station N04, observations indicate that Atlantic water extends all the way to the bottom on monthly time scales. The remaining task is therefore to determine monthly averaged depth of the Atlantic layer at stations N04 to N10 and the northern boundary of the Atlantic layer.

As discussed in H2020, the depth of the Atlantic layer at station j is based on the depth, $D_j(t)$, of the 4°C-isotherm at the station. There are periods when in situ observations (e.g., from bottom temperature loggers or PIES) can give more accurate isotherm depths, but outside of these periods, we have to rely on altimetry. Following H2020 (although with slightly changed definitions and notation), the depth of the 4°C-isotherm, $D_j(t)$, at standard station j, may be derived from:

$$D_j(t) = D_j^0 + \Gamma_j(t) + A_j \cdot cos\left[2\pi \cdot \left(t - \frac{Day_j}{365}\right)\right] + a_{h,j} \cdot h_j(t) + a_{x,j} \cdot Pc_1(t) \qquad (19)$$

where the long-term variation is given by:

$$\Gamma_j(t) = \gamma_j \cdot t + a_{TA,j} \cdot [T_A(t) - \langle T_A \rangle] \qquad (20)$$

Values for the various coefficients in Eq. (19) and Eq. (20) were derived in H2020 (e.g., their Table 5.17), where it was also demonstrated how large a fraction (R^2) was explained of the variance in the depth of the 4°C-isotherm as observed by CTD. These values are listed in the top row of all but the last column of Table 3.11.

The bottom row of Table 3.11 lists the R^2 values when using the new altimetry data. As before, we find that the new altimetry data improve the relationship for all of the standard stations. New values for the coefficients in Eq. (19) and Eq. (20) are listed in Table 3.12.

Table 3.11. All but the last columns list the fraction (R^2) of the variance of the 4°C-isotherm as observed by CTD that is explained by Eq. (19) and Eq. (20) using both the old and the new altimetry data. The last column lists explained variance by Eq. (22).

	$D_j(t)$							PcS_1
	N04	N05	N06	N07	N08	N09	N10	
Old altimetry data	0.31	0.62	0.58	0.66	0.63	0.56	0.54	0.58
New altimetry data	0.35	0.70	0.67	0.71	0.69	0.58	0.56	0.60

Table 3.12. Coefficients to use with Eq. (19) and Eq. (20) to simulate 4°C-isotherm depth at stations N04 to N10 and explained variance (R^2) of the isotherm depths from CTD.

Coeff.:	D_j^0	γ_j	$a_{TA,j}$	A_j	Day_j	$a_{h,j}$	$a_{x,j}$	R^2
Unit:	m	m/yr	m/°C	m			m	
N04:	368	1.97	0.0	25	298	1561	-61.29	0.35
N05:	261	2.33	30.6	32	294	2739	-115.92	0.70
N06:	205	3.20	44.0	45	283	2167	-106.16	0.67
N07:	162	3.16	45.1	65	262	1902	-88.02	0.71
N08:	115	3.12	30.4	56	269	1946	-78.16	0.69
N09:	59	3.00	0.0	48	262	917	0.00	0.58
N10:	48	1.21	0.0	48	270	493	0.00	0.56

In H2020 (their page 70), it was noted that the algorithms for calculating $D_j(t)$, when used for calculating 28-day averaged isotherm depth at stations N05 and N07 could reproduce the values measured by the PIES better than would be expected. The top row of Table 3.13 is copied from Table 5.15 in H2020 and one sees that the R^2 values in this table are considerably higher than the values for these two stations in the top row of Table 3.11.

We have repeated this analysis using the new altimetry data with the revised coefficients (Table 3.12) and the result is listed in the bottom row of Table 3.13. Once again, the values for R^2 increase when going from the old to the new altimetry data and coefficients. More important, perhaps, the R^2 value for isotherm depth at N05 using the new data increases from 0.70 in Table 3.11 to 0.79 in Table 3.13. For N07, the increase is from 0.71 to 0.84. *Thus, when used on 28-day averaged data, the algorithms developed from the snapshot CTD data perform considerably better than indicated by Table 3.11.*

Table 3.13. The correspondence between 28-day averaged depths of the 4°C-isotherm for stations N05 and N07 as observed by the PIES and as simulated by the expressions derived from the CTD data at the stations using both the old and the new altimetry data and coefficients. "R^2" is the variance explained by the fit. "std", "max", "min", and "avg" are the standard deviation, maximum, minimum, and average of the difference (observed – simulated), respectively.

	N05					N07				
	R^2	std	max	min	avg	R^2	std	max	min	avg
Old altimetry data:	0.77	29m	60m	-42m	1m	0.79	24m	43m	-59m	-2m
New altimetry data:	0.79	29m	42m	-54m	-6m	0.84	21m	46m	-52m	-1m

As seen in Table 3.12, the depth of the 4°C-isotherm, $D_j(t)$, can be fairly well estimated from altimetry data alone for most of the standard stations, but for station N04, this method only explains 35% of the variance, even with the new data set. In H2020, it was, however, shown that much better estimates could be obtained in periods when bottom temperature was available from the site NE (Table 2.1). With the daily averaged bottom temperature at this site denoted as $T_{NE}(t)$, the isotherm depth was determined by:

$$D_4(t) = d_{0,4} + \gamma_4 \cdot t + A_4 \cdot cos\left[2\pi \cdot \left(t - \frac{Day_4}{365}\right)\right] + a_{NE} \cdot T_{NE}(t) + b_{x,4} \cdot x(t) \qquad (21)$$

with γ_4, A_4, and Day_4 as listed in Table 3.12 and $x(t)$ as a parameter based on the altimetry data. For each choice of this parameter, the three coefficients, $d_{0,4}$, a_{NE}, and $b_{x,4}$, were determined by regression analysis on the de-trended and de-seasoned values of $D_4(t)$. Altogether, there were 47 CTD cruises in the periods with bottom temperature data at NE, from which values of $D_4(t)$ are available. With the new altimetry data, as for the old, the altimetry parameter giving the best fit was $x(t) = u_3(t)$, and, once again, we find that Eq. (21) explains a larger fraction of the variance of $D_4(t)$ when using the new altimetry data, rather than the old (Table 3.14).

Table 3.14. Explained variance (R^2) and coefficients to use with Eq. (21) to simulate 4°C-isotherm depth at station N04 with $x(t) = U_3(t)$ as well as the Root-Mean-Square (RMS) and maximal (Max) errors of the fit, based on the old and the new altimetry data, respectively.

Coeff.:	R^2	$d_{0,4}$	γ_4	A_4	Day_4	a_{NE}	$b_{x,4}$	RMS	Max
Unit:		m	m/yr	m		m/°C	s	m	m
Old altimetry:	0.66	259	1.97	25	298	32.1	-323	36	101
New altimetry:	0.71	264	1.97	25	298	31.2	-290	34	104

The choice of the 4°C-isotherm as the deep boundary of Atlantic water (H2015) was made because a temperature of 4°C is approximately midway between the temperatures of pure Atlantic (≈8°C) and Arctic (≈0°C) water. As the core temperature of Atlantic water changes, this argument no longer holds. To get the depth of the Atlantic water extent at any of the standard stations, we therefore follow H2020 and subtract 15 m, from the 4°C-isotherm depth for every degree that the Atlantic water core is warmer than 8°C and add it for every degree that the Atlantic water core is colder than 8°C.

In Sect. 7 of H2020, the northern boundary of Atlantic water on the section was defined to be where the "normalized maximum salinity", $S_j^*(t)$, falls below 35.075. It was furthermore argued that $S_j^*(t)$ on monthly time scales may be approximated by its first EOF mode:

$$S_j^*(t) \cong \langle S_j^* \rangle + M_j^{S1} \cdot PcS_1(t) \qquad (22)$$

where M_j^{S1} is the first spatial mode of $S_j^*(t)$ while $PcS_1(t)$ is its principal component. A multiple regression analysis was found to link this principal component to the first principal component of the altimetry data, which we in this report have termed $Pc_1(t)$. As shown in the top row of the last column of Table 3.11, this regression equation could explain 58% of the variance with the old altimetry data. The regression has now been re-done with the new altimetry data. The explained variance increased to 60% and the new relationship is:

$$S_j^*(t) \cong \langle S_j^* \rangle + M_j^{S1} \cdot [-0.211 \cdot h_6(t) + 1.035 \cdot Pc_1(t) + 0.905] \qquad (23)$$

3.5 Heat transport and transport-averaged properties

In addition to volume transport, we also calculate monthly averaged values for heat transport relative to 0°C, $\Omega(t)$, and transport-averaged values for temperature, $\Theta(t)$, and salinity, $\Psi(t)$, defined as:

$$\Omega(t) = \rho \cdot C \cdot \sum_{k=2}^{7} \sum_{z=1m}^{500m} U_k(z,t) \cdot T_k(z,t) \cdot W_k(z,t) \qquad (24a)$$

$$\Theta(t) = \frac{\sum_{k=2}^{7} \sum_{z=1m}^{500m} U_k(z,t) \cdot T_k(z,t) \cdot W_k(z,t)}{Q(t)} \qquad (24b)$$

$$\Psi(t) = \frac{\sum_{k=2}^{7} \sum_{z=1m}^{500m} U_k(z,t) \cdot S_k(z,t) \cdot W_k(z,t)}{Q(t)} \qquad (24c)$$

where $\rho \cdot C$ is the heat capacity per cubic meter while $T_k(z,t)$ and $S_k(z,t)$ are the temperature and salinity at depth z and time t horizontally averaged across altimetry interval k. Algorithms for determining $T_k(z,t)$ and $S_k(z,t)$ are discussed in H2015. Their dependence on altimetry is through $D_j(t)$ and $Pc_1(t)$. No further modifications of the algorithms are therefore needed for switching to the new altimetry data set.

3.6 Comparing transport values from the old and the new altimetry data

To illustrate the effects of the new altimetry data set on the four monitoring parameters, Table 3.15 compares monthly averaged values (1993 – 2018) based on the old data set with the coefficients previously reported (H2015, H2019, and H2020) against the values based on the new data set with the coefficients derived in this report. The two versions are highly correlated and all differences are small.

Table 3.15. Comparison between monthly averaged characteristics of the four monitoring parameters as calculated from the old altimetry data set with the old coefficients and the new data set with the new coefficients documented in this report.

	Correl.	Average		Std dev.		Minimum		Maximum	
Parameter	coeff.	Old	New	Old	New	Old	New	Old	New
Vol. transp.(Sv):	0.969***	3.82	3.81	0.55	0.54	2.10	2.43	5.66	5.69
Heat transp.(TW):	0.973***	124.44	124.74	19.61	19.30	71.30	74.20	191.20	192.20
Average Temp(°C):	0.998***	7.38	7.39	0.70	0.71	5.90	5.93	8.72	8.74
Average Salinity:	0.998***	35.13	35.13	0.05	0.05	35.00	35.00	35.21	35.21

References

Hansen, B., Hátún, H., Kristiansen, R., Olsen, S. M., and Østerhus, S.: Stability and forcing of the Iceland-Faroe inflow of water, heat, and salt to the Arctic, Ocean Science, 6, 1013-1026, 10.5194/os-6-1013-2010, 2010.

Hansen, B., Larsen, K. M. H., Hátún, H., Olsen, S. M., Gierisch, A. M. U., Østerhus, S., and Ólafsdóttir, S. R.: The Iceland–Faroe warm-water flow towards the Arctic estimated from satellite altimetry and in situ observations, Ocean Sci., 19, 1225–1252, https://doi.org/10.5194/os-19-1225-2023, 2023.

H2015: Hansen, B., Larsen, K. M. H., Hátún, H., Kristiansen, R., Mortensen, E., and Østerhus, S.: Transport of volume, heat, and salt towards the Arctic in the Faroe Current 1993–2013, Ocean Science, 11, 743-757, 10.5194/os-11-743-2015, 2015.

H2019: Hansen, B., Larsen, K. M. H., and Hátún, H.: Monitoring the velocity structure of the Faroe Current, Havstovan Technical Report Nr.: 19-01. TechRep1901.pdf (hav.fo).

H2020: Hansen, B., Larsen, K. M. H., Hátún, H., and Østerhus, S.: Atlantic water extent on the Faroe Current monitoring section, Havstovan Technical Report Nr.: 20-03. TechRep2003.pdf (hav.fo).

Pyper, B. J. and Peterman, R. M.: Comparison of methods to account for autocorrelation in correlation analyses of fish data, Can. J. Fish. Aquat. Sci., 55, 2127–2140, https://doi.org/10.1139/f98-104, 1998.

von Storch H.: Misuses of Statistical Analysis in Climate Research. In: von Storch, H., Navarra, A. (eds) Analysis of Climate Variability. Springer, Berlin, Heidelberg, 1999.

Appendix: Summary of equations, algorithms, and coefficients

Monitoring section

In situ observations are obtained along a section following 6°05'W longitude. CTD observations mainly from 14 standard stations N01 at 62°20'N to N14 at 64°30'N.

Altimetry data: Delayed-mode SLA values are downloaded for 8 grid points, labelled A_1 to A_8, along 6.125°W from 62.125°N to 63.875°N.

File structure

Main directory: O:\UMHVDATA\TIMESER\Faroe Current\

Subdirectories:

Altimetry\
TS_Atl\
Atl_extent\
DATA\

Notation

Sea level anomaly (SLA) at point A_k at time *t*:	$H_k(t)$
Difference in Sea level anomaly between A_k and A_{k+1} (A_k - A_{k+1}) at time *t*:	$\Delta H_k(t)$
Eastward surface velocity anomaly averaged between A_k and A_{k+1} at time *t*:	$u_k(t)$
Altimetric offset (to get absolute surface velocity between A_k and A_{k+1}):	U_k^0
Eastward surface velocity averaged between A_k and A_{k+1} at time *t*:	$U_k(0,t)$
Eastward velocity at depth *z* averaged between A_k and A_{k+1} at time *t*:	$U_k(z,t)$
Temperature at depth *z* averaged between A_k and A_{k+1} at time *t*:	$T_k(z,t)$
Salinity at depth *z* averaged between A_k and A_{k+1} at time *t*:	$S_k(z,t)$
Bottom depth (in m) between 62.33 and 64.50 in steps of 0.01° :	$D_B(latitude)$
Width of Atlantic layer at depth *z* between A_k and A_{k+1} at time *t*:	$W_k(z,t)$
Depth of the 4°C-isotherm (in m) at standard station *j* at time *t*:	$D_j(t)$
The northward boundary of Atlantic water on the section at time *t*:	$B_j(t)$
Heat capacity per cubic meter:	$\rho \cdot C$
Three-year running mean of the deseasoned average temperature 101-150m at N03:	$T_A(t)$
Three-year running mean of the deseas. salinity of the core of Atlantic water on the section:	$S_A(t)$

Altimetry parameters

The file "samlad.txt" on subdirectory DATA\ contains 16 parameters for every day:

Eight SLA values: $H_k(t)$ for k = 1 to 8

Seven surface velocity anomalies: $u_k(t) = \frac{g}{f \cdot L} \cdot [H_k(t) - H_{k+1}(t)]$

The principal component $Pc_1(t)$ associated with the first EOF mode $M_1(k)$:

$$Pc_1(t) = \frac{\sum_k [H_k(t) - \langle H_k \rangle] \cdot M_1(k)}{\sum_k M_1(k) \cdot M_1(k)}$$

Monitoring parameters

The files "Transport_m.txt" and "Transport_y.txt" on the main directory present monthly and annually averaged values for:

Volume transport: $Q(t) = \sum_{k=2}^{7} \sum_{z=1m}^{500m} U_k(z,t) \cdot W_k(z,t)$

Heat transport: $\Omega(t) = \rho \cdot C \cdot \sum_{k=2}^{7} \sum_{z=1m}^{500m} U_k(z,t) \cdot T_k(z,t) \cdot W_k(z,t)$

Transport-averaged temperature: $\Theta(t) = \frac{\sum_{k=2}^{7} \sum_{z=1m}^{500m} U_k(z,t) \cdot T_k(z,t) \cdot W_k(z,t)}{Q(t)}$

Transport-averaged salinity: $\Psi(t) = \frac{\sum_{k=2}^{7} \sum_{z=1m}^{500m} U_k(z,t) \cdot S_k(z,t) \cdot W_k(z,t)}{Q(t)}$

Determining velocity

Velocity in altimetry interval *k* at depth *z* and time *t* is determined as:

$$U_k(z,t) = \Phi_{k,m}(z) \cdot U_k(0,t) = \Phi_{k,m}(z) \cdot \left[\frac{g}{f \cdot L} \cdot \Delta H_k(t) + U_k^0\right]$$

The values for U_k^0 (in cm s^{-1}) are stored in the file "DATA\Ubar.txt" and listed below:

Interval:	A_2-A_3	A_3-A_4	A_4-A_5	A_5-A_6	A_6-A_7	A_7-A_8
U_k^0:	12.5	21.7	18.0	10	9.5	2

The values $\Phi_{k,m}(z)$ are stored as arrays (z=1:600, m=1:12) in six files, one for each altimetry interval *k*=2 to 7: "DATA\Uprof_2.txt" to "DATA\Uprof_7.txt".

Determining the depth of the 4°C-isotherm from altimetry alone

The 4°C-isotherm depth at standard station *j* for time *t* (measured in years) is:

$$D_j(t) = D_j^0 + \gamma_j \cdot t + a_{TA,j} \cdot [T_A(t) - \langle T_A \rangle] + A_j \cdot cos\left[2\pi \cdot \left(t - \frac{Day_j}{365}\right)\right] + a_{h,j} \cdot h_j(t) + a_{x,j} \cdot Pc_1(t)$$

The coefficients are stored in "Atl_extent\Sim_coeff.txt" and have the values listed below

Coeff.:	D_j^0	γ_j	$a_{TA,j}$	A_j	Day_j	$a_{h,j}$	$a_{x,j}$
Unit:	m	m/yr	m/°C	m			m
N04:	368	1.97	0.0	25	298	1561	-61.29
N05:	261	2.33	30.6	32	294	2739	-115.92
N06:	205	3.20	44.0	45	283	2167	-106.16
N07:	162	3.16	45.1	65	262	1902	-88.02
N08:	115	3.12	30.4	56	269	1946	-78.16
N09:	59	3.00	0.0	48	262	917	0.00
N10:	48	1.21	0.0	48	270	493	0.00

Determining the depth of the 4°C-isotherm at N04 from bottom temperature and altimetry

In periods when daily averaged bottom temperature at site NE, $T_{NE}(t)$, is available, determination of the 4°C-isotherm depth at station N04 is improved by the equation:

$$D_4(t) = d_{0,4} + \gamma_4 \cdot t + A_4 \cdot cos\left[2\pi \cdot \left(t - \frac{Day_4}{365}\right)\right] + a_{NE} \cdot T_{NE}(t) + b_{x,4} \cdot u_1(t)$$

with the coefficients listed in the table below:

Coeff.:	$d_{0,4}$	γ_4	A_4	Day_4	a_{NE}	$b_{x,4}$
Unit:	m	m/yr	m		m/°C	s
New altimetry:	264	1.97	25	298	31.2	-290

Determining the depth of the Atlantic layer from "adjusted" 4°C-isotherm depth

In order to adjust for changing Atlantic water core temperature, $T_A(t)$, the depth of the Atlantic layer at station j for time t, $D_j^{Atl}(t)$, is determined from the 4°C-isotherm depth at the station, $D_j(t)$, by:

$$D_j^{Atl}(t) = D_j(t) - \alpha_{DT} \cdot [T_A(t) - T_A^0]$$

where α_{DT} = 15 m/°C and T_A^0 = 8°C.

Determining the northward extent of the Atlantic water layer

The northern boundary of Atlantic water on the section, $B_j(t)$, is a real number between 4 and 10, which is in units of standard stations (e.g., $B_j(t)$ = 7.5 means that the boundary is midway between N07 and N08). It is defined to be where the "normalized maximum salinity", $S_j^*(t)$, falls below 35.075 where:

$$S_j^*(t) \cong \langle S_j^* \rangle + M_j^{S1} \cdot [-0.211 \cdot h_6(t) + 1.035 \cdot Pc_1(\mathrm{t}) + 0.905]$$

The values for M_j^{S1} are stored in "Atl_extent\Salt_modes.txt".

Determining the temperature distribution on the section

The temperature at depth z on standard station j for time t (in years) is found as:

$$T_j(z,t) = T_j^0(z) + A_j^T(z) \cdot \cos\left[2\pi \cdot \left(t - \frac{Day_j^T(z)}{365}\right)\right] + a_j^T(z) \cdot [T_A(t) - \{T_A\}] + b_j^T(z) \cdot x_j(t) + c_j^T(z)$$

where: $x_j(t) = \begin{cases} Pc_1(t) & for\ j < 4 \\ D_j(t) & for\ j \geq 4 \end{cases}$

All the coefficients are stored as arrays (z=1:600,j=2:11) on subdirectory DATA\

$T_j^0(z)$	is stored in file: "Avg_temp.txt"
$A_j^T(z)$	is stored in file: "amp_temp.txt"
$Day_j^T(z)$	is stored in file: "phs_temp.txt"
$a_j^T(z)$	is stored in file: "a2.txt"
$b_j^T(z)$	is stored in file: "b2.txt"
$c_j^T(z)$	is stored in file: "c2.txt"

Determining the salinity distribution on the section

The salinity at depth *z* on standard station *j* for time *t* (in years) is found as:

$$S_j(z,t) = a_j^S(z) \cdot [S_A(t) - \{S_A\}] + b_j^S(z) \cdot x_j(t) + c_j^S(z)$$

where: $x_j(t) = \begin{cases} Pc_1(t) & for\ j < 4 \\ D_j(t) & for\ j \geq 4 \end{cases}$

All the coefficients are stored as arrays (z=1:600,j=2:11) on subdirectory DATA\

$a_j^S(z)$	is stored in file: "a2s.txt"
$b_j^S(z)$	is stored in file: "b2s.txt"
$c_j^S(z)$	is stored in file: "c2s.txt"

Algorithms

Calculations of monthly and annually averaged values for the four monitoring parameters are carried out in five steps on the main directory “O:\UMHVDATA\TIMESER\Faroe Current\” or one of its subdirectories.

Step 1: Prepare altimetry data on subdirectory “Altimetry\”:

Load updated altimetry data and generate the file “samlad.txt” with the 16 altimetry parameters using the Matlab script “les_altim.m” and the Fortran program “samlad.for”. After checking, “samlad.txt” is copied to subdirectory “DATA\”.

Step 2: Generate file with 3-year running mean Atlantic TS on subdirectory “TS_Atl\”:

The list of CTD cruises, "cruises.txt" is updated and 3-year running means are generated with Fortran program “ger_TS.for” and stored in file "Atl3.txt". After checking, “Atl3.txt” is copied to subdirectory “DATA\”.

Step 3: Update additional in-situ data:

If there are new bottom temperature data at NE, update “NE.txt" on subdirectory “DATA\”.
If new PIES data are available, update 'isoth_day" files on subdirectory "Atl_extent\"

Step 4: Generate file "boundary.txt" with Atlantic water extent on subdirectory "Atl_extent\":

This is carried out by a command file “update.bat” that runs five Fortran programs in sequence:

“Sim_Alt.for” generates the file “Sim_Alt.txt” with daily values for $D_j(t)$ for j = 4 to 10 based on altimetry alone.

“Sim_PIES.for” generates the file “Sim_combined.txt” from “Sim_Alt.txt” by replacing values for standard stations and days that have been observed by PIES.

“Sim_N04_NE.for” generates the file “Sim_N04_NE.txt” with $D_4(t)$ based on bottom temperature at site NE for days with observations at this site.

“Sim_combine.for” generates the file “D4C_N04_N10.txt” from “Sim_combined.txt” by replacing values for $D_4(t)$ in “Sim_N04_NE.txt”.

“boundary.for” generates the file “boundary.txt”, which contains the best estimates of $D_j(t)$ for j = 4 to 10 and the northern boundary for Atlantic water, $B_j(t)$, for every day in the altimetry period.

After checking, “boundary.txt” is copied to the main directory “O:\UMHVDATA\TIMESER\Faroe Current\”.

Step 5: Calculate and store final time series on "O:\UMHVDATA\TIMESER\Faroe Current\"
This is carried out by the Fortran program "Transport_2022.for".

Step 5-A: Call a series of subroutines that load parameters and coefficients:

subroutine "load_Alt.for" loads the sixteen altimetry parameters for every day from file "DATA\samlad.txt". It loads the U_k^0 values from file "DATA\Ubar.txt" and calculates daily absolute surface velocities for each altimetry interval k = 2 to 7. It also loads bottom depth $D_B(latitude)$.

subroutine "load_TS.for" loads 3-year running mean temperature and salinity, $T_A(t)$ and $S_A(t)$, and also all the coefficients needed to calculate the temperature and salinity distributions on the section, $T_j(z,t)$ and $S_j(z,t)$ for every day.

subroutine "load_dco.for" loads the values for $\Phi_{k,m}(z)$ that are stored as arrays (z=1:600, m=1:12) in six files, one for each altimetry interval k=2 to 7: "DATA\Uprof_2.txt" to "DATA\Uprof_7.txt".

subroutine "load_bound.for" loads daily values for the 4°C-isotherm depth, $D_j(t)$ for j = 4 to 10, and for the northern boundary of Atlantic water, $B_j(t)$, for every day in the altimetry period from the file "boundary.txt".

Step 5-B: Calculate monthly averages for $U_k(0,t)$, $W_k(z,t)$, $T_k(z,t)\cdot W_k(z,t)$, and $S_k(z,t)\cdot W_k(z,t)$.

For every day in the altimetry interval, the depth of the boundary is **adjusted** to correct for changing Atlantic core temperature, $T_A(t)$. Then five subroutine calls are made for the specified day:

subroutine "get_w.for" calculates the width, $W_k(z,t)$, of all altimetry intervals k (k = 2 to 7) at all depths depth z (z = 1 m to z = 600 m) for the specified time (day) t. The width is 1 above the boundary (for the southernmost interval, 2, it is ½), which is bottom or the adjusted 4°C isotherm and it is 0 below the boundary or north of the northern boundary. Where the boundary goes through depth z in interval k, $W_k(z,t)$ is the fraction above the boundary. To do this, the subroutine first generates an array "*d(m)*" with m = 1 to 168 containing the deep boundary for that day in latitudinal increments of 0.01°. So, m = 1 corresponds to latitude 62.1667° (N01) and m = 168 corresponds to latitude 63.8333° (N10). In the southern part of the section, *d(m)* is set to the bottom depth minus 5 m (to exclude the bottom boundary layer). North of N04, *d(m)* is made equal to the depth of the adjusted 4°C isotherm. South of N04, the deep boundary between N04 and N05 is extrapolated southwards until it hits bottom, although at most ± 39 m from the boundary depth at N04. Once *d(m)* is determined for the specified day, the subroutine goes through all the altimetry intervals and for each then scans from z = 1 m to z = 600 m to determine how large a fraction of the interval is above *d(m)* at the depth.

subroutine "get_TS.for" calculates the temperature, $T_j(z,t)$, and salinity, $S_j(z,t)$, on each standard station j (j = 2 to 11) and all depths z for the specified time (day) t by using the coefficients loaded by "load_TS.for" in the equations listed above.

subroutine "get_wT.for" with parameter *itbd* = 0 calculates the product, $T_k(z,t) \cdot W_k(z,t)$, for all altimetry intervals k (k = 2 to 7) and all depths z (z = 1 m to z = 600 m) for the specified time (day) t. This call is used for heat transport, which is for all the water warmer than 0°C. The subroutine therefore first calculates the depth of the 0°C-isotherm at each standard station from N04 northwards. Then the steps in "get_w.for" are repeated to find *d(m)* along the section. By linear interpolation of $T_j(z,t)$ between standard stations, an array "*tsw(m,z)*" is calculated with the temperature for the specified day at every depth z = 1 m to z = 600 m and with m = 1 to 168 representing latitude in increments of 0.01°. Once *d(m)* and *tsw(m,z)* are determined for the specified day, the subroutine goes through all the altimetry intervals and for each of them scans from z = 1 m to z = 600 m to determine how large a fraction of the interval is above *d(m)* at the depth and to average *tsw(m,z)* in that part.

subroutine "get_wT.for" with parameter *itbd* = 4 is used to calculate transport-averaged temperature. It is the same subroutine as referred to above, but only integrates down to the adjusted 4°C-isotherm.

subroutine "get_wS.for" is used to calculate transport-averaged salinity down to the adjusted 4°C-isotherm. It is similar to "get_wT.for" with parameter *itbd* = 4, only with $T_j(z,t)$ replaced by $S_j(z,t)$.

With the outputs from these subroutines, monthly sums are accumulated and averages are calculated for $U_k(0,t)$, $W_k(z,t)$, $T_k(z,t) \cdot W_k(z,t)$, and $S_k(z,t) \cdot W_k(z,t)$ for every month in the period.

Step 5-C: Calculate and store monthly averaged values for the monitoring parameters.

Open output file for monthly values, "DATA\Transport_m.txt" and write header.

For every month in the period and every altimetry interval (k = 2 to 7), **integrate** vertically (z = 1 m to z = 500 m) monthly averaged surface velocity $U_k(0,t)$ multiplied by $\Phi_{k,m}(z)$ and a scaling factor to derive volume transport of Atlantic water.

Similarly, integrate to get sums to determine heat transport and transport-averaged values for temperature and salinity.

Write monthly values for the four monitoring parameters to the output file.

Step 5-D: Calculate and store annually averaged values for the monitoring parameters.

Open output file for annual values, "DATA\Transport_y.txt" and write header.

Calculate and write annual averages from the monthly averages.

Nóatún 1
FO-100 Tórshavn
Faroe Islands

Tel +298 35 39 00
hav@hav.fo
www.hav.fo